Published in final edited form as:
Nanotechnology. 2007 January 24; 18(9): 095601. doi:10.1088/0957-4484/18/9/095601.

A New Solution Route to Hydrogen Terminated Silicon Nanoparticles: Synthesis, Functionalization, and Water Stability

Xiaoming Zhang[1,2], **Doinita Neiner**[1], **Shizhong Wang**[1,2], **Angelique Y. Louie**[2,*], and **Susan M. Kauzlarich**[1,*]

[1]Department of Chemistry, University of California, Davis, CA 95616

[2]Department of Biomedical Engineering, University of California, Davis, CA 95616

Abstract

Hydrogen capped silicon nanoparticles with strong blue photoluminescence were synthesized by the metathesis reaction of sodium silicide, NaSi, with NH_4Br. The hydrogen capped Si nanoparticles were further terminated with octyl groups and then coated with a polymer to render them water soluble. The nanoparticles were characterized by TEM, FT-IR, UV-VIS absorption, and photoluminescence. The Si nanoparticles were shown to have an average diameter of 3.9 ±1.3 nm and exhibited room-temperature photoluminescence with a peak maximum at 438 nm with a quantum efficiency of 32% in hexane and 18% in water; the emission was stable in ambient air for up to 2 months. These nanoparticles could hold great potential as a non-heavy element containing quantum dot for applications in biology.

1. Introduction

The observation of strong visible emission in porous silicon has triggered substantial interest in exploring the synthesis and characterization of silicon nanoparticles [1, 2]. Unlike bulk silicon, the emission from nanoscaled silicon can be attributed to radiative recombination of carriers confined in silicon nanoparticles and its color can be suitably modified by changing the nanoparticle size. This particular size-dependent optical characteristic has been proposed to lead to important applications for the nanoparticles in the applications of optoelectronic devices [3-5], light-emitting devices [6], and photopumped tunable lasers.[7] Recently, luminescent silicon nanoparticles have been prepared by a variety of physical and chemical approaches such as electrochemical etching [8], ion implantation [9], thermal vaporization [10], laser ablation [11], and gas phase decomposition of silanes [12, 13]. Solution chemistry routes are attractive because particle size and surface chemistry can be controlled simultaneously. These strategies include sonochemical reduction of $Si(OEt)_4$, reduction of $SiCl_4$ using Zintl salts [14], and other reductive routes [15-19].

Due to their biocompatibility, high photoluminescence quantum efficiency, and stability against photobleaching, silicon nanoparticles are expected to be an ideal candidate for replacing fluorescent dyes in many biological assays and fluorescence imaging techniques

*Corresponding authors: aylouie@ucdavis.edu, smkauzlarich@ucdavis.edu.

[20-23, 5]. Several groups have carried out surface functionalization of silicon for biological applications. Tilley et al. [18] recently reported the synthesis of allylamine capped silicon quantum dots and demonstrated their potential as a fluorophore in HeLa cells. The emission is in the blue region of the spectrum. The quantum yield of these silicon nanoparticles is reported to be 10% in water and stable for several months. Ruckenstein el. al. [20] synthesized poly(acrylic acid) grafted silicon nanoparticles via laser induced pyrolysis with a CO_2 laser followed by graft polymerization. The nanoparticles were obtained from the CO_2 laser heating of a silane gas mixture and then the particles were HF etched to reduce size and to passivate their surface. Finally, the surface of the nanoparticles were grafted with an acrylic acid polymer to make them water-soluble. The surface-modified nanoparticles exhibited bright fluorescence images in Chinese hamster ovary (CHO) cells and provided higher resistance to photobleaching than commonly used organic dyes. The quantum yield of these silicon nanoparticles is reported to be initially 24% in water with red emission and degrade slowly over a period of several weeks [20]. Most recently, Si-rich suboxide particles have been employed as a starting material for Si nanoparticles [24]. This synthetic method also employs an etching process, combining HF/HNO_3 with sonication to remove the oxide and reduce the size of the particles. Silicon nanoparticles have been proposed as better quantum dots for *in vivo* applications [20, 2] and for photodynamic therapy [25]. While the etching processes described above does not hinder the applications of these nanoparticles, a direct method for preparing hydrogen terminated silicon nanoparticles with less processing would be an improvement.

In this study, we describe a convenient method for the preparation of water-soluble silicon nanoparticles with intense photoluminescence. The synthesis method involves reaction of the Zintl salt (NaSi) with ammonium bromide [26, 27]. The formation reaction proceeds via a chemical “metathesis” process, in which hydride-covered elemental silicon are formed with several by-products, e.g. NH_3, H_2, and NaBr. The yield is quantitative and results in a hydrogen terminated silicon nanoparticle. The hydride-covered silicon nanoparticles can be modified further by a hydrosilylation process to form chemically robust Si-C bonds on the surface [28]. Finally, a biocompatible and synthetically convenient polymer [29] can be coated on the alkyl-terminated silicon nanoparticles to make the latter water soluble, while retaining a high quantum yield (QY).

2. Experimental section

Materials

N,N-Dimethylformamide (DMF), (EMD chemicals, >99%) was degassed, and distilled over sodium metal under reduced pressure. Ammonium bromide (Aldrich, >99.99%) was dried at 100 °C under vacuum and stored in glove box. HPLC-grade chloroform (Aldrich), and HPLC-grade water (Fisher) were used as received without further purification. All chemicals were handled either in a N_2-filled glovebox or on a Schlenk line using standard anaerobic and anhydrous techniques. Glassware was dried overnight at 120 °C and transferred hot into an N_2-filled glovebox. Unless otherwise stated, all samples are oxygen-sensitive and precautions must be taken to avoid exposure to oxygen.

NaSi was synthesized according to the literature [30, 31]. To synthesize silicon nanoparticles, 100 ml N,N-Dimethylformamide (DMF) was added via cannula to NaSi (0.1 g, 2 mmol) in a three-neck bottle and heated to reflux, and formed a black opaque suspension. NH_4Br (0.2 g, 2 mmol) was added and the mixture was stirred for 48 hours resulting in a brown solution. The reaction mixture was allowed to cool to room temperature. After removing the black precipitate, 40 μl of 0.072M H_2PtCl_6 solution was added by anaerobic syringe followed by 2 ml octene. The solution was stirred overnight and the solvent was then removed via vacuum evaporation. The resulting product obtained was dissolved in chloroform. The chloroform solution was purified by extraction with a water/hexane mixture to remove any impurities such as NaBr, the Pt catalyst, and any unreacted NH_4Br. The hexane extract was further centrifuged to acquire a clear and light yellow solution. The light yellow solution can be dried to obtain a light-yellow solid, and the solid can be resuspended in many organic solvents, such as hexane, ethanol, and chloroform.

Water-soluble silicon nanoparticles were prepared, as outlined in Scheme I, by capping the nanoparticles with an amphiphilic polymer of octylamine-modified poly(acrylic acid). The polymer was prepared following the reported literature method with minor modifications [32, 29]. Typically, 10 g of poly(acrylic acid, sodium salt) was diluted two-fold in water and acidified with 150 mL of 12 N hydrochloric acid. This solution was then dialyzed against sodium chloride in water for about 48 h. The solution was then heated to approximately 60°C under vacuum to remove the water. After fully dried, 72 mg of the polymer was dissolved in 30 mL of dimethylformamide (DMF) and reacted with 75 μL of n-octylamine, using 100 μL of ethyl-3-dimethyl amino propyl carbodiimide (EDC) as a cross-linking reagent (45% of carboxyl groups in the polymer were modified). The reaction system was placed under an Ar atmosphere and stirred overnight. Solvent was then removed by vacuum, and the resulting oily product was dissolved in methanol and dialyzed with water to remove excess EDC and other byproducts. After vacuum drying, 20 mg of the product was then dissolved in 10 mL of chloroform. To this polymer solution, 5 mg silicon nanoparticles in 10 mL of chloroform was added. The solvent was pumped off under vacuum. The polymer-coated octyl capped silicon nanoparticles were readily dissolved in 5 mL of water, and then centrifuged in a dialysis tube to remove any excess polymer.

The products were characterized by FTIR, TEM and photoluminescence spectroscopy. Transmission Electron Microscopy (Phillips CM-120, operating at 80 kV) was used to analyze the size distribution of the prepared product. TEM samples were prepared by dipping holey-carbon-coated, 400-mesh electron microscope grids into the hexane colloid solution and drying them at 120 °C overnight. Energy dispersive X-ray spectroscopy (EDS) was performed on JOEL 2500SE with an accelerating voltage of 200 kV. The corresponding histogram of silicon nanoparticles size based on a survey of 870 particles from different regions of the grid. UV-vis and PL spectra of silicon colloid solution were obtained on a Cary 100 Bio spectrometer (Varian) and FluoroMax-3P fluorometer, respectively. ^1H NMR (300 MHz) spectra were recorded on a Varian Mercury 300 instrument on the dispersions of the octyl capped Si particles, polymer, and polymer-coated octyl capped Si nanoparticles in deuterated chloroform (see Supporting Information). The FT-IR spectra were collected on a Shimadzu IR Prestige 21 spectrophotometer by dropping the hexane colloid on a KBr plate and allowing the solvent to evaporate. Photoluminescence quantum yield was obtained by

comparison of the PL intensity of a nanoparticle sample with that of the solution of quinine sulfate (laser grade) in 0.1M H_2SO_4 solution. Literature value of 0.54 was taken for the room-temperature PL efficiency of quinine sulfate in 0.1M H_2SO_4 solution [33]. Isolated samples were dissolved in chloroform or water and measured in a standard 1-cm quartz cell with controlled optical densities below 0.10 at the excitation wavelength.

3. Results and Discussion

Figure 1 shows the X-ray powder diffraction pattern obtained from the solid product before hydrosilation. The diffraction pattern shows two broad diffraction peaks at approximately 28° and 52°, consistent with observations for amorphous silicon [26, 34, 35]. The peaks at 28°, 47°, 58° could correspond to the (111), (220), (311) reflections of crystalline silicon and the positions and indices are shown in Figure 1. As can be seen from the comparison of the calculated vs. experimental intensities, the experimental intensity of (220) reflection is weaker than what would be expected, if we assumed that the entire sample was crystalline. Therefore, the product is most likely a mixture of amorphous and crystalline silicon. Belomoin et. al. examined the structural change of Si nanocrystals as a function of size and found that small nanoparticles (1.0 nm diameter) may also provide a similar diffraction pattern with two broad peaks at approximately 28 ° and 52 ° [36]. However, because the average particle size of the sample is approximately 4 nm in diameter (see discussion from TEM below), the diffraction pattern is best interpreted as due to mainly amorphous Si with a smaller amount of crystalline silicon present [34]. No evidence of silicon suboxide, which gives a diffraction peak at 21°, is observed [37].

Figure 2 shows a typical transmission electron (TEM) micrograph, along with the size distribution and energy dispersive X-ray spectroscopy (EDS). The image indicates that the average diameter of silicon nanoparticles is 3.9 ± 1.3 nm as shown in Figure 2b. No aggregation is observed in the TEM image. The narrow size distribution and high dispersivity indicate that the hydrophobic interaction between long aliphatic chains effectively stabilize the resulting silicon nanoparticles [38]. To further ensure that particles are composed of silicon, energy dispersive X-ray spectroscopy (EDS) was performed on the particles. In Figure 1c, the peaks associated with silicon, carbon, and oxygen are observed. The copper peak is attributed to the copper support of the TEM grid.

Figure 3 shows FT-IR spectra for hydrogen-terminated Si particles (curve A) and octyl capped Si particles (curve B). For curve A, the peak at 2085 cm^{-1} can be attributed to the Si-H stretching mode. This is consistent with the hydrogen termination of the nanoparticles. The peaks in the region of 1000-1200 cm^{-1} correspond to Si–OR asymmetric stretching vibration and indicates that some oxidization of the silicon nanoparticles has occurred. For curve B, strong peaks corresponding to alkyl C-H_x bonds at 2960, 2920, 2860, and 1463 cm^{-1} appear after treatment with octane [19]. The peak observed at 1258 cm^{-1} is attributed symmetric bending of Si-CH_2. The absence of Si-H bond at 2085 cm^{-1} and the formation of Si-C bond at 1273 cm^{-1} provide clear evidence of the expected hydrosilylation product. The peaks at 1732 cm^{-1} may be attributed to C=C double bond from octene. Presumably some octene molecules are absorbed on the surface of the Si nanoparticles.

Optical absorption and photoluminescence spectroscopy were used to investigate the optical properties of the silicon nanoparticles (Figure 4). The UV-VIS absorption spectrum of a hexane solution of Si nanoparticles shows an absorption onset at about 450 nm extending toward a narrow maximum 275 nm. The photoluminescence spectra show a relatively narrow region of intense luminescence with maximum intensity from ~420-450 nm, with excitation from 360-400 nm. The maximum intensity emission spectrum is centered at 438 nm with an excitation wavelength of 380 nm. Changes in the excitation wavelength excite different size populations of nanoparticles, resulting in the varying emission wavelengths observed. Though some questions about origin and mechanism of the fluorescence in Si nanoparticles remain actively debated [39, 40], the large increase in energy of the photoluminescence relative to the band gap of Si (e.g., 1.1 eV for bulk Si) and the linear shift in photoluminescence wavelength with excitation wavelength point to quantum confinement [4]. From these data, we can obtain the photoluminescence quantum yield. The quantum yields of up to 28% were obtained relative to the standard quinine sulfate in 0.1 M H_2SO_4 solution.

The Si nanoparticles were rendered water soluble by coating with octylamine-modified poly(acrylic) acid (average molecular weight = 8,000) as illustrated in Scheme 1., ^{1}H NMR was performed to investigate the surface functionalization and coverage of Si nanoparticles, as shown in Figure S1 (supporting information). The spectra are similar to those of references [41, 42]. No new peaks were observed in polymer-coated Si nanoparticles and this indicates there are no bond formed between Si nanoparticles and the polymer.

Figure 5 shows the normalized photoluminescence of the nanoparticles before (black, in hexane) and after coating (blue, in water). Almost no shift or broadening is observed in the emission spectra in the two media. Quantum yield, however, decreased and was ~2 fold lower in water. This suggests that surface reconstruction or disorder due to hydrolysis of the surface may be important. Generally, oxidation can greatly affect the electronic charge distribution in the silicon nanoparticles and consequently lower the band gap [43]. Since the emission energy is unaffected, the lower quantum yield may be attributed to dipolar interactions between water and the nanoparticles [44]. In this paper, the polymer coating did decrease this interaction between silicon and water and allow both high solubility and high quantum yield. Other nanoparticles, such as CdSe/ZnS with the same type of surface coating typically demonstrate a quantum yield of 10-18% in water [45], and the value obtained herein for Si nanoparticle in water is comparable to that reported in the literature [18]. After 2-3 months, quantum yields are similar which indicates that the silicon nanoparticles are stable in water. The inset in the top left corner of Figure 5 shows the characteristic bright blue luminescence from a cuvette of polymer-capped silicon nanoparticles in water when excited with a commercial hand held low-intensity UV lamp. Interestingly, the emission is similar to what is reported for very small nanoparticles (~2 nm) of silicon capped in a similar manner [46, 5]. These nanoparticles could be used as nanovectors that are surface-modified with biological materials such as antibodies, which can be used to target a specific marker in cancer cells [47, 5]. Blue emission is not ideal for *in vivo* imaging but is suitable for biological research. In addition, recent results in photodynamic therapy utilizing Si

nanoparticles provides further incentive to optimize a high yield, easy synthetic method for Si nanoparticles with a chemical assesible surface [25].

In conclusion, we have reported the synthesis of water-soluble, luminescent silicon nanoparticles with high quantum yield. The surface of the silicon nanoparticles was modified by octane and capped with hydrophilic polymers. Such water-soluble silicon nanoparticles displayed strong photoluminescence in the blue region of the visible spectrum with an 18% quantum yield. The attached organic molecules allow not only water solubility but also high stability, and coating has little adverse effect on the optical properties of nanoparticles. This synthesis route is simple and thus offers great opportunity for scaled-up preparation of semiconductor materials. The highly PL stable and non-aggregated Si-particles may provide a good alternative to Cd based quantum dots for biomedical applications. Current efforts focus on producing nanoparticles with stable green and red emission with high quantum yields by this method.

Supplementary Material

Refer to Web version on PubMed Central for supplementary material.

Acknowledgments

This work was supported by the NIH (HL081108-01). The authors thank Andrea M. Goforth for providing the ^{1}H NMR spectra.

References

1. Canham LT. Appl. Phys. Lett. 1990; 57:1046.
2. Veinot JGC. Chem. Commun. 2006:4160.
3. Fauchet PM. Materialstoday. 2005:26. January.
4. Liu Q, Kauzlarich SM. Mater. Sci. Eng. B. 2002; 96:72.
5. Buriak JM. Phil. Trans. R. Soc. A. 2006; 364:217. [PubMed: 18272462]
6. Lee S, Cho WJ, Chin CS, Han IK, Choi WJ, Park YJ, Song JD, Lee JI. Jpn. J. Appl. Phys. 2004; 43:L784.
7. Canham LT. Appl. Phys. Lett. 1993; 63:337.
8. Belomoin G, Therrien J, Nayfeh M. Appl. Phys. Lett. 2000; 77:779.
9. Kobayashi T, Endoh T, Fukuda H, Nomura S, SaKai A, Ueda Y. Appl. Phys. Lett. 1997; 71:1195.
10. Buuren TV, Dinh LN, Chase LL, Siekhaus WJ, Terminello LJ. Phys. Rev. Lett. 1998; 80:3803.
11. Hata K, Yoshida S, Fujita M, Yasuda S, Makimura T, Murakami K, Shigekawa H. J. Phys. Chem. B. 2001; 105:10842.
12. Vial JC, Bsiesy A, Gaspard F, He'rino R, Ligeon M, Muller F, Romestain R, MacFarlane R. Phys. ReV. B. 1992; 45:14171.
13. Mangolinia L, Thimsen E, Kortshagen U. Nano Letters. 2005; 5:655. [PubMed: 15826104]
14. Bley RA, Kauzlarich SM. J. Am. Chem. Soc. 1996; 118:12461.
15. Pettigrew KA, Liu Q, Power PP, Kauzlarich SM. Chem. Mater. 2003; 15:4005.
16. Baldwin RK, Pettigrew KA, Garno JC, Power PP, Liu G-y, Kauzlarich SM. J. Am. Chem. Soc. 2002; 124:1150. [PubMed: 11841266]
17. Baldwin RK, Provencio KA, Ratai E, Augustine MP, Kauzlarich SM. Chem. Commun. 2002:1822.
18. Warner JH, Hoshino A, Yamamoto K, Tilley RD. Angew. Chem. Int. Ed. 2005; 44:4550.
19. Yang C-S, Bley RA, Kauzlarich SM, Lee HWH, Delgado GR. J. Am. Chem. Soc. 1999; 121:5191.

20. Li ZF, Ruckenstein E. Nano Lett. 2004; 4:1463.
21. Wang L, Reipa V, Blasic J. Bioconjugate Chem. 2004; 15:409.
22. Yoshinobu T, Ecken H, Ismail ABM, Iwasaki H, Luth H, Schoning M. J. Electrochim. Acta. 2001; 47:259.
23. Delerue C, Allan G, Lannoo M. Phys. Rev. B. 1993; 48:11024.
24. Sato S, Swihart MT. Chemistry of Materials. 2006; 18:4083.
25. Timoshenko VY, Kudryavtsev AA, Osminkina LA, Vorontsov AS, Ryabchikov YV, Belogorokhov IA, Kovalev D, Kashkarov PK. JETP Letters. 2006; 83:423.
26. McMillan PF, Gryko J, Bull C, Arledge R, Kenyon AJ, Cressey BA. J. Solid State Chem. 2005; 178:937.
27. Neiner D, Chiu HW, Kauzlarich SM. J. Am. Chem. Soc. 2006; 128:11016. [PubMed: 16925406]
28. Buriak JM. Chem. Rev. 2002; 102:1271. [PubMed: 11996538]
29. Wu X, Liu H, Liu J, Haley KN, Treadway JA, Larson JP, Ge N, Peale F, Bruchez MP. Nat. Biotechnol. 2003; 21:41. [PubMed: 12459735]
30. Mayeri D, Phillips BL, Augustine MP, Kauzlarich SM. Chem. Mater. 2001; 13:765.
31. NaSi can also be purchased from SigNa Chemistry L. New York: p. 933-4101.http://www.signachem.com
32. Wang KT, Iliopoulos I, Audebert R. Polym. Bull. 1988; 20:577.
33. Demas JN, Crosby GA. J. Phys. Chem. 1971; 75:991.
34. Neiner D, Chiu HW, Kauzlarich SM. J. Am. Chem. Soc. 2006; 128:11016. [PubMed: 16925406]
35. Kapaklis V, Politis C, Poulopoulos P, Schweiss P. Applied Physics Letters. 2005; 87:123114.
36. Belomoin G, Alsalhi M, Aql AA, Nayfeh MH. J. Appl. Phys. 2004; 95:5019.
37. Liu, S-m; Sato, S.; Kimura, K. Langmuir. 2005; 21:6324. [PubMed: 15982038]
38. Yamanoi Y, Yonezawa T, Shirahata N, Nishihara H. Langmuir. 2004; 20:1054.
39. Takagahara T, Takeda K. Phys. Rev. B. 1992; 46:15578.
40. Klimov VI, Schwarz CJ, McBranch DW, White CW. Appl. Phys. Lett. 1998; 73:2603.
41. Hua F, Swihart MT, Ruckenstein E. Langmuir. 2005; 21:6054. [PubMed: 15952860]
42. Hua FJ, Erogbogbo F, Swihart MT, Ruckenstein E. Langmuir. 2006; 22:4363. [PubMed: 16618188]
43. Zhou Z, Brus L, Friesner R. Nano Lett. 2003; 3:163.
44. Lauerhaas JM, Credo GM, Heinrich JL, Sailor MJ. J. Am. Chem. Soc. 1992; 114:1911.
45. Gerion D, Pinaud F, Williams SC, Parak WJ, Zanchet D, Weiss S, Alivisatos AP. J. Phys. Chem. B. 2001; 105:8861.
46. Tilley RD, Warner JH, Yamamoto K, Matsui I, Fujimori H. Chem. Commun. 2005:1833.
47. Cohen MH, Melnik K, Boiarski AA, Ferrari M, Martin FJ. Biomed Microdevices. 2003; 5:253.

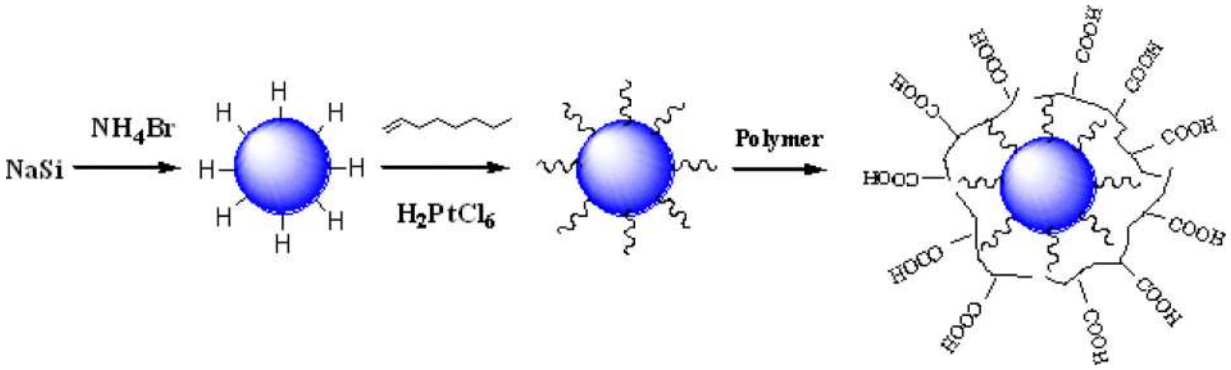

Scheme 1.

Synthetic route for generation of water soluble silicon nanoparticles. Synthesized by a "metathesis" reaction of NaSi and NH_4Br, the hydride-covered silicon nanoparticles can be modified by a hydrosilylation process to form Si-C bond on the surface. Finally, an amphiphilic polymer of octylamine-modified poly(acrylic acid) can be coated on the alkyl-terminated silicon nanoparticles to render water soluble with a high quantum yield.

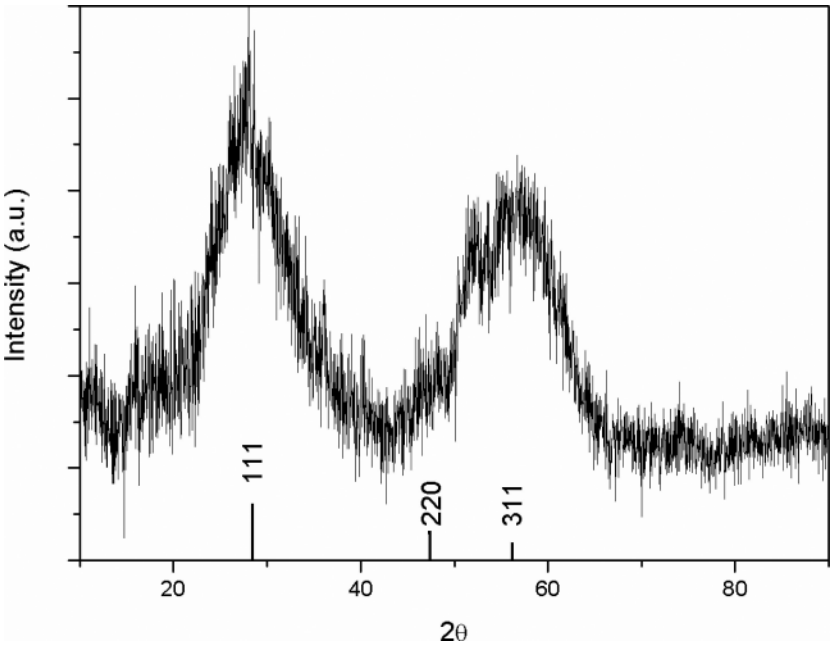

Figure 1.
X-ray powder diffraction of the silicon nanoparticles with hydrogen termination. Calculated peaks with indices for crystalline silicon are provided.

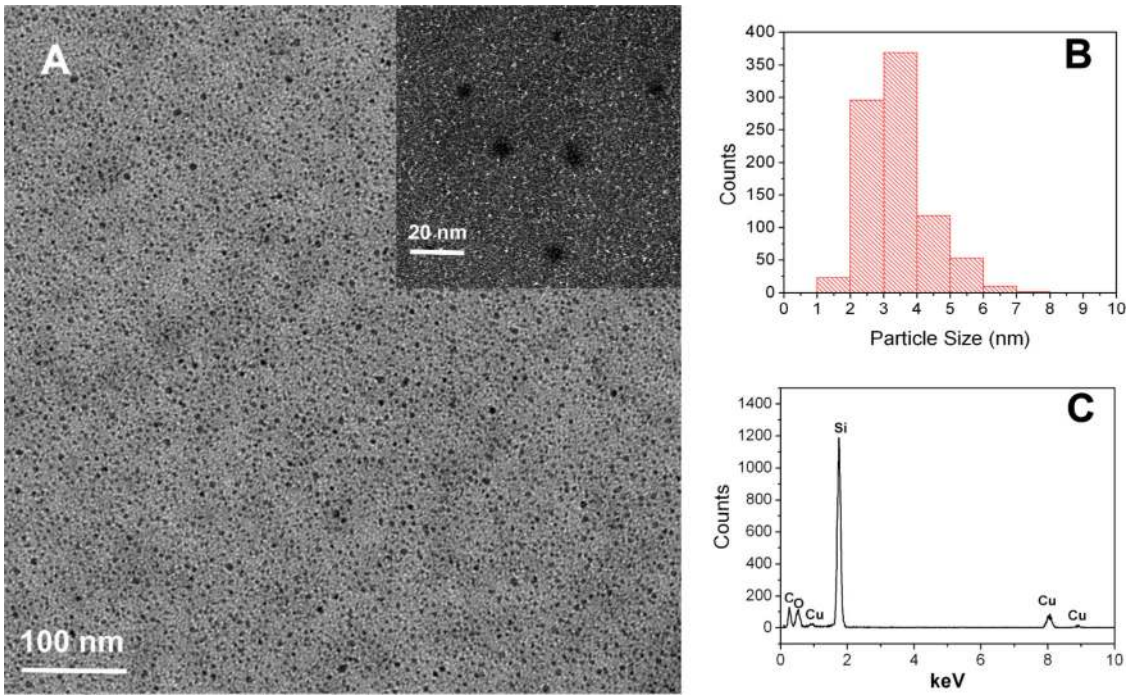

Figure 2.

(a) TEM image of silicon nanoparticles. The inset shows an enlarged view. (b) The corresponding histogram of silicon nanoparticles size based on a survey of 870 particles from different regions of the grid. (c) Energy dispersive X-ray spectroscopy (EDS) performed on the nanoparticles, copper peaks result from the TEM grid.

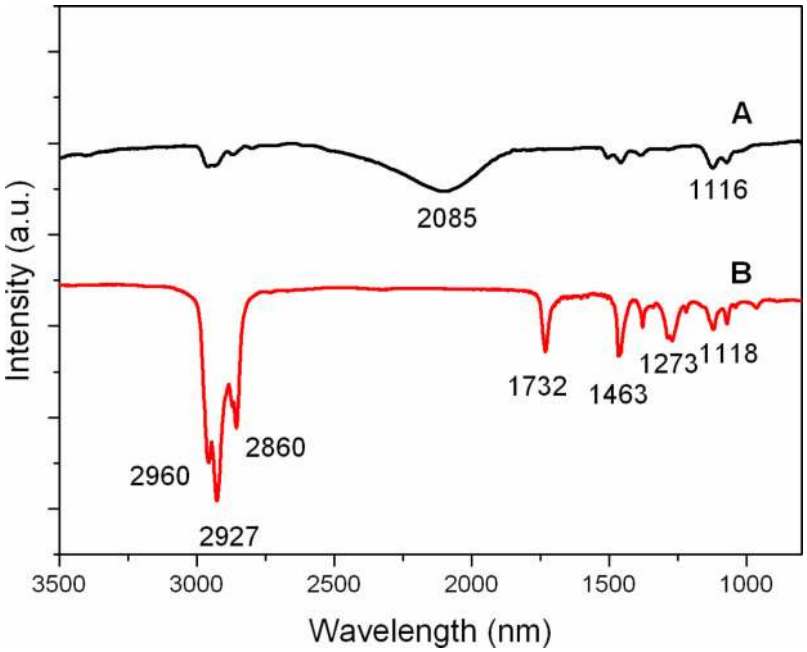

Figure 3.

FT-IR spectra of as-prepared hydrogen terminated silicon nanoparticles (curve A) and octyl capped silicon nanopaprticles (curve B). The wavenumbers for the corresponding stretches are indicated.

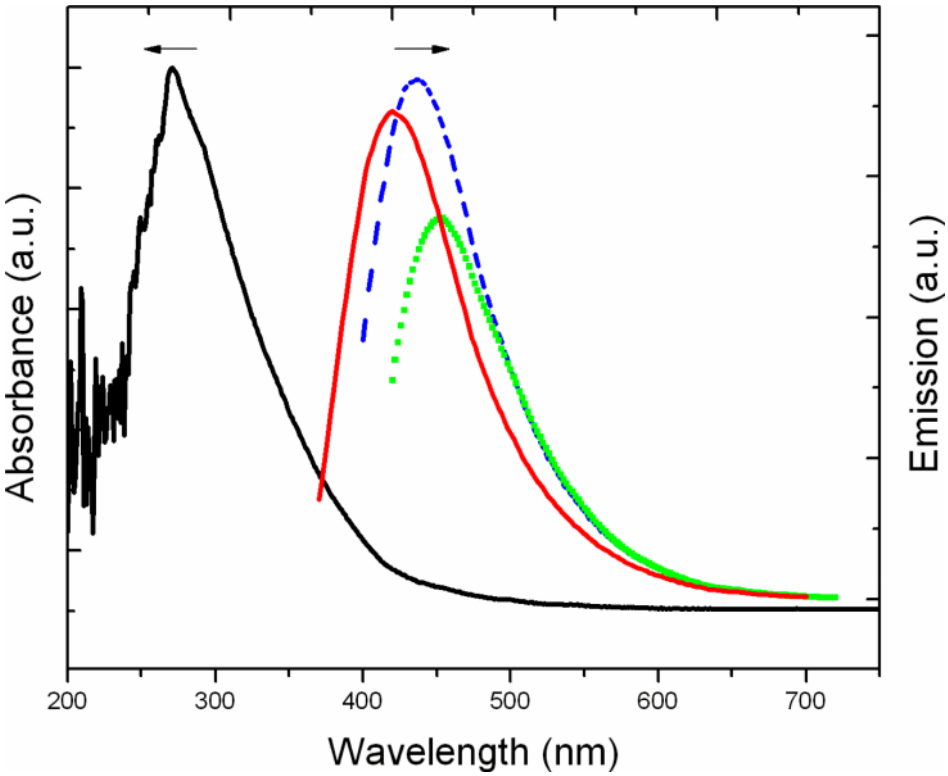

Figure 4.
Absorption spectra (black) and room temperature PL spectra of silicon nanoparticles at different excitation wavelengths: 360 (red); 380 (blue); and 400 (green).

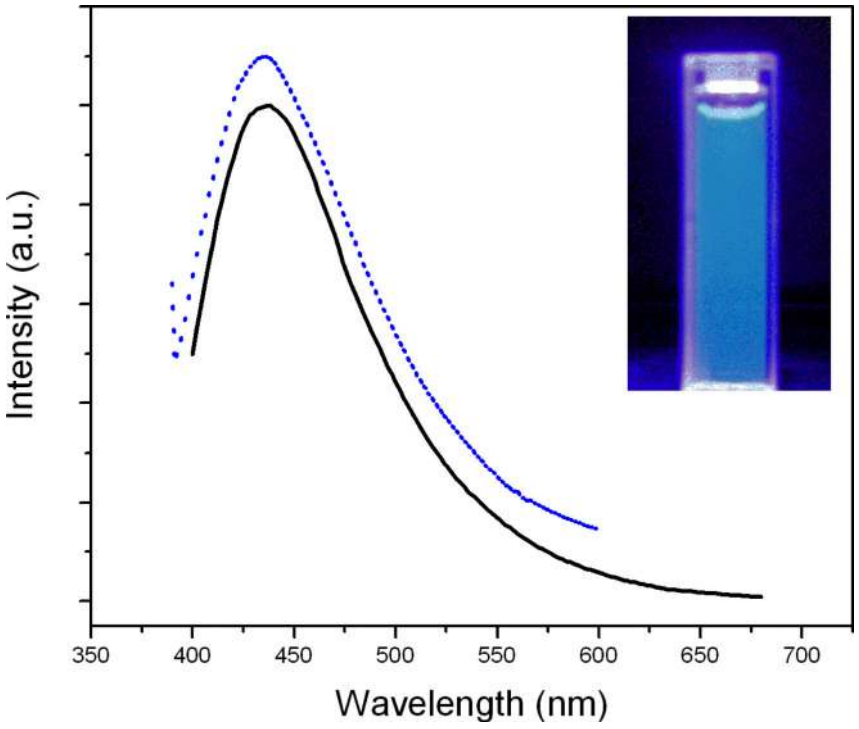

Figure 5.

Normalized photoluminescence spectra (excitation wavelength at 380 nm) of silicon nanoparticles, in hexane (black) and in water (blue). Inset: fluorescence from a cuvette of polymer-coated silicon nanoparticles in water when excited with a UV lamp.